Stem Cell Reports, Volume *12*

Supplemental Information

iPSC-Derived Brain Endothelium Exhibits Stable, Long-Term Barrier Function in Perfused Hydrogel Scaffolds

Shannon L. Faley, Emma H. Neal, Jason X. Wang, Allison M. Bosworth, Callie M. Weber, Kylie M. Balotin, Ethan S. Lippmann, and Leon M. Bellan

Supplemental Figures

Figure S1. Effects of hydrogel composition upon EC attachment. Related to Figure 1.

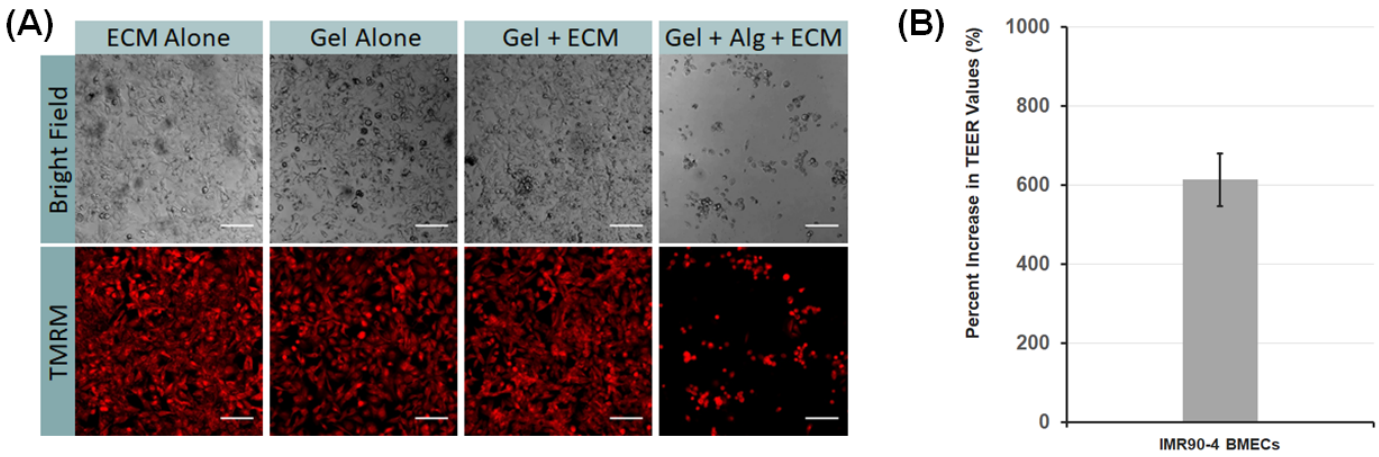

(A) IMR90-4-derived BMECs were seeded in 6-well plates coated with collagen/fibronectin solution (ECM Alone) or thin hydrogels comprised of enzymatically crosslinked 10% gelatin (Gel Alone), 10% gelatin treated with collagen/fibronectin (Gel + ECM), or 10% gelatin/0.25% Sodium-alginate treated with collagen/fibronectin solution (Gel+Alg+ECM). Gelatin/alginate hydrogels were crosslinked with mTG suspended in a 30 mM $CaCl_2$ solution. Cells were labeled with 1 µM mitochondrial stain, tertramethylrhodamineester (TMRM, Thermo Fisher) to identify live cells in fluorescence images. Scale bar represent 100 µm. **(B)** Graph illustrating the percent increase in maximum TEER values obtained from IMR90-4-derived BMECs, initially differentiated at starting iPSC densities of 120,000 or 150,000 cells per well (Hollmann et al., 2017), cultured on 7.5% gelatin hydrogels treated with collagen/fibronectin solution relative to non-treated hydrogels. Results reflects data compiled from 3 independent seedings from the 120,000 cells/well condition (N=3 Transwell filters per seeding, or N=9 total) and 2 independent seedings from the 150,000 cells/well condition (N=3 Transwell filters per seeding, or N=6 total). Error bars indicate ± 1 SD.

Figure S2. Permeability measurement data. Related to Figure 2.

(A)

Static Culture		Average	SD	*N1*	*N2*	*N3*
Day 1	IMR90-4 (D1)	1.22389E-07	5.9755E-08	1.6227E-07	5.4123E-08	1.5077E-07
	HUVEC	1.18354E-05	3.9553E-06	1.0857E-05	9.66E-06	1.499E-05
	uVas	4.95379E-07	3.6477E-07	2.7962E-07	2.9571E-07	9.1081E-07
Day 7	IMR90-4 (D1)	4.55303E-07	2.0771E-07	4.0714E-07	6.819E-07	2.7686E-07
	HUVEC	6.9814E-06	1.7915E-05	8.7731E-07	1.158E-06	1.8909E-05
	uVas	1.30489E-06	3.0378E-07	1.0538E-06	1.217E-06	1.6438E-06
Day 14	IMR90-4 (D2)	1.82649E-07	1.0749E-07	3.0547E-07	1.5376E-07	9.3933E-08
	IMR90-4 (D1)	2.15148E-06	3.6044E-06	1.8057E-07	4.1224E-06	3.1932E-06
	HUVEC	1.95006E-05	3.6499E-05	2.7554E-05	2.9059E-05	1.8894E-06
	uVas	1.23186E-06	2.1343E-07	1.2382E-06	1.017E-06	1.4438E-06
	CC3	1.98234E-07	1.019E-07	9.247E-08	2.9578E-07	2.0645E-07

(B)

Perfused Culture		Average	SD	*N1*	*N2*	*N3*
Day 1	IMR90-4 (D1)	1.94198E-07	1.8145E-08	2.0702E-07	1.8138E-07	1.8057E-07
	HUVEC	1.19041E-05	2.0004E-05	2.0793E-05	3.0155E-06	2.8306E-05
	uVas	5.95E-07	2.25E-07	5.30E-07	4.16E-07	7.56E-07
Day 7	IMR90-4 (D1)	1.40283E-07	8.6925E-08	9.3816E-08	2.4042E-07	8.6609E-08
	HUVEC	7.61697E-06	6.4097E-06	8.5993E-06	1.1918E-05	2.334E-06
	uVas	5.30E-07	1.04E-08	1.3171E-06	1.6912E-06	1.1606E-06
Day 14	IMR90-4 (D2)	3.21978E-09	1.733E-09	5.2198E-09	2.2743E-09	2.1652E-09
	IMR90-4 (D1)	4.27278E-08	3E-08	4.7624E-08	6.9907E-08	1.0653E-08
	HUVEC	2.28263E-05	1.1676E-05	1.8236E-05	2.2458E-05	2.7785E-05
	uVas	1.56426E-06	1.3679E-06	2.9212E-06	1.3171E-06	4.5456E-07
	CC3	4.24561E-08	2.7269E-08	2.5754E-08	2.7707E-08	7.3907E-08

Calculated values for 3 kDa dextran in **(A)** static and **(B)** perfused channels lined with HUVEC, μVas, IMR90-4-derived BMECs, or CC3-derived BMECs. Two explicitly different IMR90-4-derived BMEC batches were used to directly compare biological variance (denoted as D1 and D2).

Figure S3. qPCR analysis of BBB related markers. Related to Figure 2.

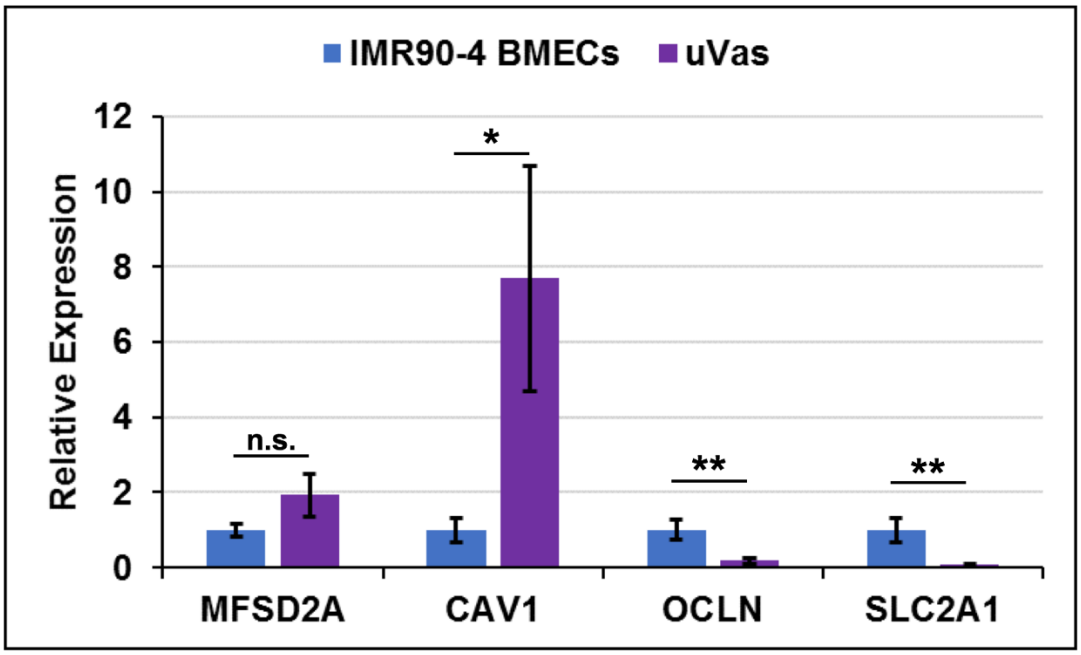

Relative expression of *MSFD2A*, *CAV1* (Caveolin-1), *OCLN* (Occludin), and *SLC2A1* (GLUT-1) in IMR90-4-derived BMECs versus μVas cells isolated from channels after 14 days of continual perfusion. *GAPDH* was used as the housekeeping gene. N=3 independent biological replicates for each condition. Error bars indicate ± 1 SD. Statistical significance was calculated using the student's unpaired t-test: *, $p<0.05$; **, $p<0.01$; n.s., $p>0.05$.

Figure S4. Permeability measurements from 3D stop-flow conditions and 2D Transwell controls. Related to Figure 2.

(A)

K (cm/s) (x10^{-7})		
Day 7	**BMEC**	6.4 ± 3.2
	HUVEC	114 ± 4.1
Day 14	**BMEC**	5.8 ± 2.2
	HUVEC	109 ± 15.4

(B)

K (cm/s) (x10^{-7})		
μVas	**Fluorescein**	507 ± 436
	3 kDa dextran	13.9 ± 2.7
	Albumin	0.03 ± 0.05
BMEC	**Fluorescein**	168 ± 50.8
	3 kDa dextran	102 ± 9.7
	Albumin	0.02 ± 0.001

(A) Permeability of CC3-derived BMECs and RFP-HUVECs to 3 kDa dextran when cultured on Transwell filters. **(B)** Permeability values from diffusion of sodium fluorescein, 3 kDa dextran, and albumin across cell monolayers after 14 days under stop-flow conditions. IMR90-4-derived BMECs and μVas were subjected to 10 min of media perfusion per day at 100 μl/min for 14 days. For all experiments, data represent mean ± SD calculated from N=3 independent biological replicates.

Figure S5. Perfusion system assembly components. Related to Figure 1.

(A)

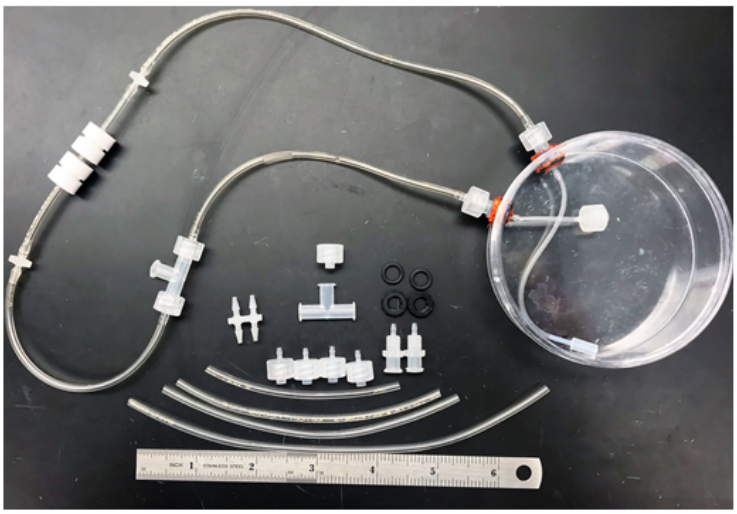

(B)

Materials	Volume
Tygon tubing - 1/16th in. (ID) x 22 in (L)	1.5 ml
Petri dish - 100 mm (D) x 30 mm (H)	40 ml
(4) 1/16th in. polypropylene Male barbed luer	
(2) 1/16th in. polypropylene barb to barb connector	
(2) Polypropylene 28 UNF threaded barb (1/16th in.) bulkhead	
(1) Polypropylene t-junction	
(1) Polypropylene luer cap	
(2) VIKON o-rings	
(2) PVDF bulkead locking nuts	

(A) Fully assembled fluidic culture apparatus used for continual and stop-flow perfusion experiments. **(B)** List of individual components used to construct perfusion system. The total volume of medium within the perfusion system during an experiment is estimated to be between 40-45 ml.

Figure S6. Measuring diffusion coefficients in gelatin matrix using FRAP analysis. Related to Figure 2 and Experimental Procedures.

(A.)

Diffusion Coefficient in 10% Gelatin (μ^2/s)	
Fluorescein (332 Da)	69.3 ± 1
3K Cascade Blue Dextran	22.5 ± 0.6
3K AF 680 Dextran	20.9 ± 0.3
10K Oregon Green Dextran	12.6 ± 0.5
Fluorescein-BSA (66K Da)	4.04 ± 0.3

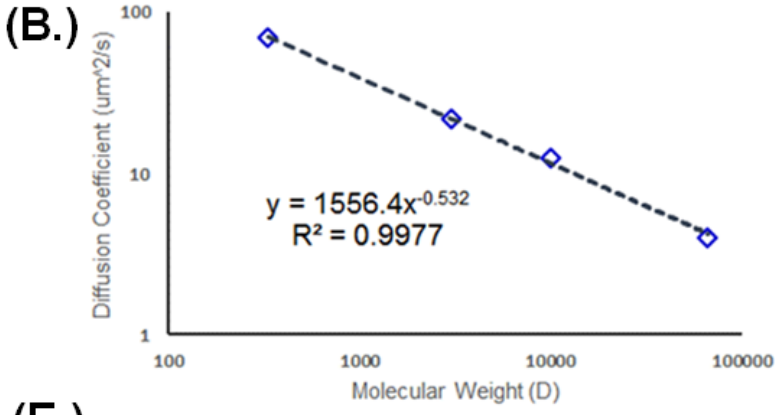

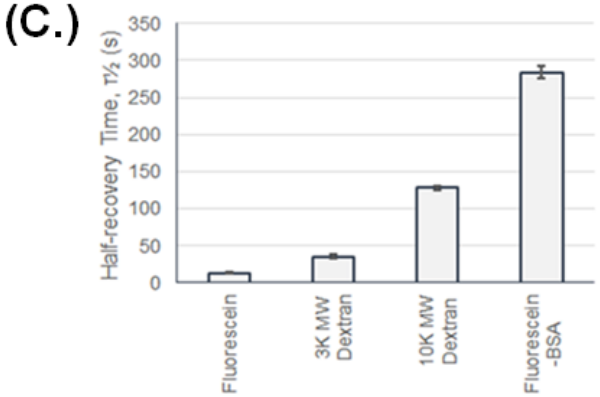

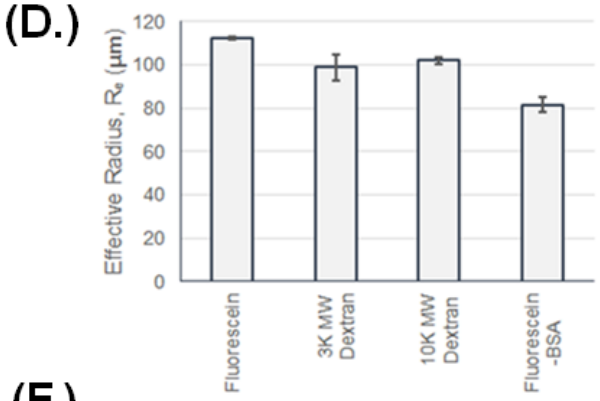

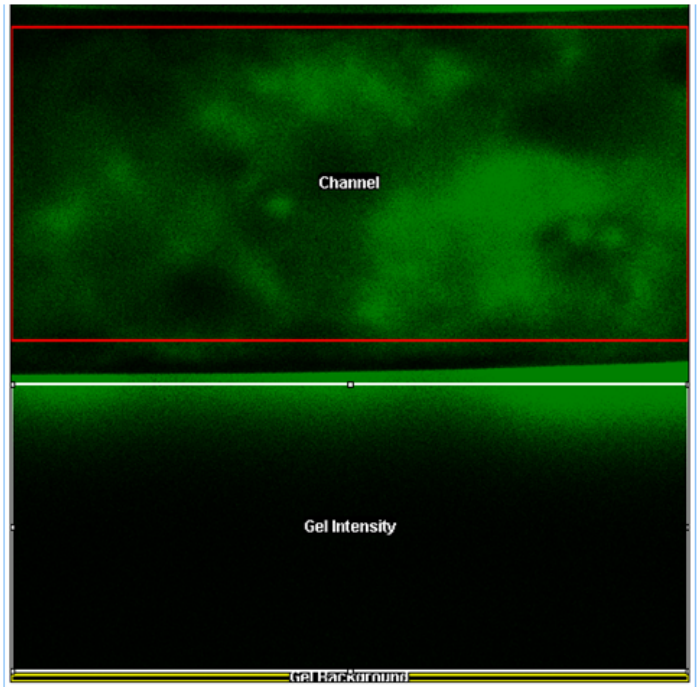

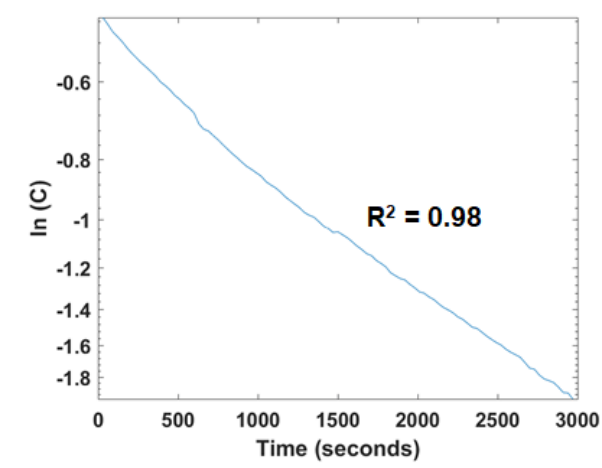

(A) Calculated diffusion coefficient values based upon N ≥ 3 experiments. **(B)** Comparison of molecular weight to calculated diffusion coefficient. Slope of the line is -0.53 with an R-squared value of 0.997, which correlates with previous reports (Arrio-Dupont et al., 1996). **(C)** Half-recovery times of fluorescein and dextran FRAP experiments. **(D)** Effective radius measurements of bleached samples. Error bars indicate ± 1 SD. **(E)** Screen capture illustrating ROI delineations for image processing in Fiji. **(F)** Representative plot of Log (C) versus time generated from intensity profiles in Matlab. The slope of the linear plot corresponds to Lambda (λ) and is used in Equation S4 to calculate the diffusion coefficient.

Supplemental Tables

Table S1. Global RNA expression in IMR90-4-derived BMECs cultured in channels for 1 day under static conditions and 14 days under perfused conditions. Related to Figure 2. Data are compiled in an accompanying spreadsheet.

Supplemental Movies

Movie 1. One-hour time-lapse showing diffusion of 3 kDa dextran across channels lined with RFP-HUVECs cultured under static conditions for 7 days. Related to Figure 2A.

Movie 2. One-hour time-lapse showing diffusion of 3 kDa dextran across channels lined with IMR90-4-derived BMECs cultured under static conditions for 7 days. Related to Figure 2A.

Movie 3. Two-hour time-lapse showing diffusion of fluorescein across channels lined with μVas cells cultured for 14 days under perfusion. Related to Figure 3A.

Movie 4. Two-hour time-lapse showing diffusion of fluorescein across channels lined with IMR90-4-derived BMECs cultured for 14 days under perfusion. Related to Figure 3A.

Supplemental Experimental Procedures

FRAP Measurements. In order to calculate the permeability of endothelial cell layers to sodium fluorescein, dextran, and albumin based upon time lapse images, the diffusivity of each molecule in gelatin was first determined through fluorescence recovery after photobleaching (FRAP) analysis. Excellent in-depth reviews of the principles and mathematical theory for determining diffusion coefficients based upon FRAP analysis have been previously described (Axelrod et al., 1976; Braeckmans et al., 2003; Soumpasis, 1983). In summary, an intense laser beam of known dimension is used to irreversibly bleach fluorophores within the exposed sample region. The diffusion coefficient is related to the speed at which the fluorescence the bleached region recovers, dictated by the speed at which bleached compounds diffuse out of the region and are replaced by unbleached fluorophores. Hence, the diffusion coefficient is most strongly related to the size of the compounds. Potential sources of error include immobilized compounds (e.g. molecules that stick to a coverslip) and unbound fluorophore which could under- or over-estimates of diffusion coefficients. To account for this, we performed FRAP analysis in control samples using five different compounds ranging in molecular weight between ~300 to 66,000 Daltons. Using multiple compounds of varying molecular weight allowed us to verify accuracy of the FRAP method as diffusivity should relate directly to molecular weight. Our results (**Figure S6**) indicated a strong linear relationship between diffusion coefficient and molecular weight, suggesting these potential sources error having minimal impact and, thus, no further steps to introduce correction for immobile molecules or unbound fluorophores were taken.

Uniform solutions of 10% (w/v) gelatin containing 10 μg/ml fluorescein (*MW = 332 g/mol*), 125 μg/ml Cascade Blue-Dextran (*MW = 3,000 g/mol*), 125 μg/ml Alexa-Fluor 680-Dextran (*MW = 3,000 g/mol*), 0.5 mg/ml Oregon Green-Dextran (*MW = 10,000 g/mol*), or 100 μg/ml Fluorescein-BSA (*MW = 66,000 g/mol*) were crosslinked with 1% (w/v) mTG. Approximately 200 μl of crosslinked gelatin solution containing individual fluorophores was sandwiched between two glass slides (Fisher Scientific) to form a thin gelatin layer approximately 60 μm in thickness. FRAP experiments were conducted using a Zeiss LSM 710 laser scanning confocal microscope and the bleaching module included in Zen Black (Zeiss) imaging software. For each trial, 10 pre-bleach images were obtained to calculate initial fluorescence intensity. Samples were then bleached, using the zoom-bleaching function to increase efficiency, with the appropriate laser (405 nm line of 30 mW Diode laser was used to bleach Cascade Blue Dextran, the 488 nm line of 35 mW Argon laser bleached Fluorescein, Oregon Green-Dextran, and Fluorescein-BSA, and 633 nm line of 5mW HeNe laser bleached Alexa-Fluor 680-Dextran) within a central designated bleach region (diameter = 60 pixels, or ~100 μm) until the bleached intensity reached 50% of the initial fluorescence intensity. Subsequent acquisition of time series images over the course of 100-500 seconds, depending on the dye, documented the fluorescence recovery. The pinhole aperture was held at maximum for all samples. Laser power was set to maximum to effectively bleach each dye through the entire thickness (*z*-axis) of the sample, such that fluorescence recovery depended most upon diffusion along the *x*-*y* dimension. To minimize the effects of diffusion occurring during the

process of photo-bleaching from skewing calculations based upon FRAP data, image resolution was set to 512x512 pixels per frame to reduce scan time (pixel dwell = 1.58 μs).

Calculating Diffusivity from FRAP Data. Diffusion coefficients for isotropic, nonreactive solutions were calculated from FRAP data based upon Fickian diffusion, most notably outlined by Axelrod and Soumpasis (Axelrod et al., 1976; Soumpasis, 1983) and later optimized (Braeckmans et al., 2003) to account for special consideration associated with photobleaching using laser-scanning confocal microscopy. Most recently, a simplified method for extracting the diffusion coefficients from confocal laser scanning FRAP data was described according to Equation S1, where D is the diffusion coefficient ($\mu m^2/s$), R_n is the nominal radius of the laser spot, R_e is the effective radius (1/2 diameter of bleached region), and $\tau_{1/2}$ is the half-recovery time (Kang et al., 2012).

$$\textbf{Equation (S1)}: \quad D = \frac{R_n^2 + R_e^2}{8\tau_{1/2}}$$

Automated measurements performed by modified version of the freely available Frap-jython macro for ImageJ (Schindelin et al., 2012; Schneider et al., 2012) provided the half-recovery time from individual FRAP data sets and identified the "FRAP frame" where fluorescence intensity within the bleached region reached a minimum. This frame was then used to measure the effective radius (R_e) from the plot profile function in ImageJ. The nominal radius (R_n) was the same for every sample at 50 μm. Calculated diffusion coefficients based upon FRAP experiments are shown in **Figure S6**.

Diffusion Imaging Analysis. Using Fiji, each dataset was first aligned (if necessary), before identifying the coordinates defining each region of interest corresponding to the areas comprising (1) channel interior, (2) gelatin background (farthest point from channel) and (3) gelatin next to the channel were entered into a custom Fiji macro. The macro script used to obtain the intensity profiles corresponding to the aforementioned region of interest is included as **Appendix S1**. Diffusivity was then calculated based on methods previously reported (Zheng et al., 2012), first using Equation S2:

$$\textbf{Equation (S2)}: Bi = \frac{K\delta}{D_{gelatin}} = \lambda \cdot tan\lambda$$

Where Bi is the Biot number, K (cm/s) is the permeability, δ is the distance between the edge of the channel and the edge of the gel (cm), $D_{gelatin}$ (cm/s) is the diffusivity of the compound of interest (e.g. 3 kDa dextran) in gelatin, and λ is the slope of linear fit for the following relation describing the change in fluorescence intensity versus time:

$$\textbf{Equation (S3)}: \lambda = \ln\left(\Delta \frac{I_{edge} - I_{channel}}{I_{gel} - I_{channel}}\right) \cdot \frac{1}{\Delta t}$$

Where I_{edge} is the integrated fluorescence intensity profile corresponding to the edge of the gelatin scaffold (also referenced as gel background), $I_{channel}$ is the integrated fluorescence intensity profile of channel, and I_{gel} correspond to the fluorescence

intensity of the gel next to the channel (the active area of dextran diffusion). The previous two equations are combined to yield a formula for determining permeability (K):

$$\textbf{Equation (S4)}: K = \frac{D_{gelatin} \cdot \lambda \cdot \tan \lambda}{\delta}$$

The intensity profiles extracted from imaging analysis were then imported into a Matlab script to calculate the permeability of cell layers to generate a plot corresponding to Equation S3, which was used to determine λ. This value was then used in Equation S4, along with known values for $D_{gelatin}$ and distance (δ) to calculate the permeability (K) reflecting the combined permeability of the gelatin matrix and cell monolayer. The Matlab script used for these calculations is included as **Appendix S2**.

Control scaffolds comprised of channels without cells lining the channel were used to determine the permeability of the gelatin matrix alone (K_g). The permeability of the cell monolayer (K_c) was then determined using the following equation:

$$\textbf{Equation (S5)}: \quad \frac{1}{k} = \frac{1}{k_C} + \frac{1}{k_G}$$

Shear Calculations. Fluidic shear stress along the channel wall using the following equations:

$$\textbf{Equation (S6)}: V = \frac{Q}{A}$$

Where V is the mean fluid velocity (mm/s), Q is the pump flow rate, and A is the area of the channel. An average channel diameter (d) of 800 μm was used for all calculations. We then calculated wall shear rate (γ) using:

$$\textbf{Equation (S7)}: \gamma = 8 * \frac{V}{d}$$

Shear stress (τ) is then calculated by:

$$\textbf{Equation (S7)}: \tau = \gamma * \mu$$

where μ is viscosity. For all calculations, the media viscosity was approximated using the viscosity for 1X PBS, 0.01 Pa (Yeom et al., 2014).

Immunocytochemistry. At indicated time points, gelatin constructs were washed 3 times in 1X PBS, then fixed in 4% paraformaldehyde for 10 min at room temperature (RT). Fixed constructs were washed 3 times in 1X PBS at RT, then incubated in 1X PBS supplemented with 5% donkey serum overnight at 4 °C. After washing with 1X PBS at RT, samples were incubated in 1X PBS containing 1 μg/ml claudin-5 antibody (Alexa-Fluor 488 conjugate; 4C3C2; Thermo Fisher), 1 μg/ml occludin antibody (Alexa-Fluor 594 conjugate; OC-3F10; Thermo Fisher), and/or 1 μg/ml VE-Cadherin antibody (PA519612, Thermo Fisher) overnight at 4 °C. Samples were washed 3 times in 1X PBS before incubation with 1 mg/ml Alexa-Fluor 680 donkey anti-rabbit secondary antibody (Thermo Fisher) overnight at 4 °C to fluorescently label bound VE-cadherin antibodies. Unbound secondary antibody was removed by washing 5 times in 1X PBS at RT. For actin labeling,

cells were incubated with Rhodamine Phalloidin (1:1000 dilution; Thermo Fisher) for 20 min at RT prior to imaging. For nuclei labeling, cells were incubated with 1 µg/ml Hoechst (BD Bioscience) for 10 min at RT prior to imaging.

qPCR Analysis. Cells were detached from the channel surface by first washing 2 times in 1X PBS for 5 min, then incubating the entire gel in 5 ml 0.25% Trypsin-EDTA (Gibco) at 37 °C for 10 min. Gels were then washed twice with 5 ml Trypsin Neutralizing solution (Gibco), vigorously pipetting the solution through the channels to dislodge remaining cells. Each collection tube included cells collected from two channels (experimental replicates). The cell suspensions were pelleted by centrifugation at 1000 G for 5 min. The supernatant was discarded and the pellet was resuspended in 500 µl of room temperature TRIzol reagent (Thermo Fisher) for 10 min before storage at -80 °C. To extract RNA, samples were mixed with chloroform at a 1:5 v/v chloroform:TRIzol and centrifuged at 12,000×g for 15 min at 4°C. RNA was subsequently isolated from the resulting aqueous phase and reversed transcribed to cDNA via manufacturers' instructions using an RNeasy Mini Kit (Qiagen) and a High-Capacity cDNA Reverse Transcription Kit (Applied Biosystems), respectively. qPCR was performed on a BioRad CFX96 using a TaqMan Universal PCR Master Mix (Applied Biosystems), 15 ng cDNA per replicate per gene, and desired TaqMan Gene Expression Assays (Applied Biosystems) and manufacturers' specified thermocycler parameters. Gene expression was measured using N=3 biological replicates.

RNA Sequencing and Analysis. IMR90-4-derived BMECs were detached from channels and collected in TRIzol as described above. Total RNA was isolated using the Direct-zol RNA MiniPrep Plus Kit (Zymo Research) with DNase I treatment according to the manufacturer's instructions. Samples were submitted to Vanderbilt Technologies for Advanced Genomics (VANTAGE) for sequencing using an Illumina NovaSeq6000. Sequences were aligned to the human transcriptome (GRCh38) using HISAT2 (Kim et al., 2015) and a text file containing a list of known splice sites generated using the UCSC Table Browser (Karolchik et al., 2004) and hisat2_extract_splice_sites.py. Alignments were assembled using StringTie (Pertea et al., 2015), and transcript levels (FPKM values) were extracted using Ballgown (Frazee et al., 2015). Pearson correlation coefficient was calculated by generating a scatter plot of FPKM values with each sample on a separate axis and performing a linear regression of the plotted data.

Supplemental References

Arrio-Dupont, M., Cribier, S., Foucault, G., Devaux, P.F., and d'Albis, A. (1996). Diffusion of fluorescently labeled macromolecules in cultured muscle cells. Biophys. J. *70*, 2327–2332.

Axelrod, D., Koppel, D.E., Schlessinger, J., Elson, E., and Webb, W.W. (1976). Mobility measurement by analysis of fluorescence photobleaching recovery kinetics. Biophys. J. *16*, 1055–1069.

Braeckmans, K., Peeters, L., Sanders, N.N., De Smedt, S.C., and Demeester, J. (2003). Three-dimensional fluorescence recovery after photobleaching with the confocal scanning laser microscope. Biophys. J. *85*, 2240–2252.

Frazee, A.C., Pertea, G., Jaffe, A.E., Langmead, B., Salzberg, S.L., and Leek, J.T. (2015). Ballgown bridges the gap between transcriptome assembly and expression analysis. Nat. Biotechnol. *33*, 243–246.

Hollmann, E.K., Bailey, A.K., Potharazu, A.V., Neely, M.D., Bowman, A.B., and Lippmann, E.S. (2017). Accelerated differentiation of human induced pluripotent stem cells to blood-brain barrier endothelial cells. Fluids Barriers CNS *14*, 9.

Kang, M., Day, C.A., Kenworthy, A.K., and DiBenedetto, E. (2012). Simplified equation to extract diffusion coefficients from confocal FRAP data. Traffic Cph. Den. *13*, 1589–1600.

Karolchik, D., Hinrichs, A.S., Furey, T.S., Roskin, K.M., Sugnet, C.W., Haussler, D., and Kent, W.J. (2004). The UCSC Table Browser data retrieval tool. Nucleic Acids Res. *32*, D493-496.

Kim, D., Langmead, B., and Salzberg, S.L. (2015). HISAT: a fast spliced aligner with low memory requirements. Nat. Methods *12*, 357–360.

Pertea, M., Pertea, G.M., Antonescu, C.M., Chang, T.-C., Mendell, J.T., and Salzberg, S.L. (2015). StringTie enables improved reconstruction of a transcriptome from RNA-seq reads. Nat. Biotechnol. *33*, 290–295.

Schindelin, J., Arganda-Carreras, I., Frise, E., Kaynig, V., Longair, M., Pietzsch, T., Preibisch, S., Rueden, C., Saalfeld, S., Schmid, B., et al. (2012). Fiji: an open-source platform for biological-image analysis. Nat. Methods *9*, 676–682.

Schneider, C.A., Rasband, W.S., and Eliceiri, K.W. (2012). NIH Image to ImageJ: 25 years of image analysis. Nat. Methods *9*, 671–675.

Soumpasis, D.M. (1983). Theoretical analysis of fluorescence photobleaching recovery experiments. Biophys. J. *41*, 95–97.

Yeom, E., Kang, Y.J., and Lee, S.-J. (2014). Changes in velocity profile according to blood viscosity in a microchannel. Biomicrofluidics *8*.

Zheng, Y., Chen, J., Craven, M., Choi, N.W., Totorica, S., Diaz-Santana, A., Kermani, P., Hempstead, B., Fischbach-Teschl, C., López, J.A., et al. (2012). In vitro microvessels for the study of angiogenesis and thrombosis. Proc. Natl. Acad. Sci. U. S. A. *109*, 9342–9347.

Appendix: Data Analysis Macro Scripts

Appendix S1. Fiji macro script

```
//Analyze confocal timelapse data sets for permeability measurements

	//Find Background Intensity of Gelatin
	makeRectangle (0,1020, 1024, 10);
		// add roi (x, y, width, height)
	macro "Show Statistics" {
	    if (nSlices>1) run("Clear Results");
			getVoxelSize(w, h, d, unit);
		n = getSliceNumber();
		for (i=1; i<=nSlices; i++) {
		    setSlice(i);
		    getStatistics(area, mean, min, max, std);
		    row = nResults;
		    if (nSlices==1)
		        setResult("Area ("+unit+"^2)", row, area);
		        setResult("Mean ", row, mean);
		        setResult("Std ", row, std);
		        setResult("Min ", row, min);
		        setResult("Max ", row, max);
		  }
		setSlice(n);
		updateResults();
		saveAs("Results","path\\file.csv");

	//Find Intensity of Channel
	makeRectangle (0,100, 1024, 300);
		//add roi (x,y,w,h)
	macro "Show Statistics" {
	    if (nSlices>1) run("Clear Results");
			getVoxelSize(w, h, d, unit);
		n = getSliceNumber();
		for (i=1; i<=nSlices; i++) {
		    setSlice(i);
		    getStatistics(area, mean, min, max, std);
		    row = nResults;
		    if (nSlices==1)
		        setResult("Area ("+unit+"^2)", row, area);
		        setResult("Mean ", row, mean);
		        setResult("Std ", row, std);
		        setResult("Min ", row, min);
		        setResult("Max ", row, max);
		  }
		setSlice(n);
		updateResults();
		saveAs("Results", "path\\name.csv");
		  }

	//Find Intensity of Gelatin near channel
	makeRectangle (0,450, 1024, 560);
		// add roi (x, y, w,h)
	macro "Show Statistics" {
	    if (nSlices>1) run("Clear Results");
			getVoxelSize(w, h, d, unit);
		n = getSliceNumber();
		for (i=1; i<=nSlices; i++) {
		    setSlice(i);
		    getStatistics(area, mean, min, max, std);
		    row = nResults;
		    if (nSlices==1)
		        setResult("Area ("+unit+"^2)", row, area);
		        setResult("Mean ", row, mean);
		        setResult("Std ", row, std);
		        setResult("Min ", row, min);
		        setResult("Max ", row, max);
		  }
		setSlice(n);
		updateResults();
		saveAs("Results","path\\filename.csv");
	}

	//Analyze Time Series
	makeLine(0,512,1024,512,1);
		//add line of interest
		//(x1,y1,x2,y2,width)
	macro "Stack profile Data" {
	    if (!(selectionType()==0 || selectionType==5 ||
	selectionType==6))
		exit("Line or Rectangle Selection Required");
		setBatchMode(true);
		  run("Plot Profile");
		  Plot.getValues(x, y);
		  run("Clear Results");
		  for (i=0; i<x.length; i++)
	    setResult("x", i, x[i]);
		   close();
	    n = nSlices;
		  for (slice=1; slice<=n; slice++) {
			showProgress(slice, n);
			setSlice(slice);
			profile = getProfile();
			sliceLabel = toString(slice);
			sliceData = split("\n");
				if (sliceData.length>0) {
					line0 = sliceData[0];
						if
	(lengthOf(sliceLabel) > 0)

		  sliceLabel = sliceLabel+ " ("+ line0 + ")";
		  }
			for (i=0; i<profile.length; i++)
				setResult(sliceLabel, i,
	profile[i]);
	  }
		  setBatchMode(false);
		  updateResults;
		  saveAs("Results", "path\\filename.csv");
```

Appendix S2. Matlab code

```
%% Calculate permeability from confocal imaging datasets

    Dgelatin=20.9 %From FRAP Data 10k=12.6, 3k=20.9
    Distance_microns = 1120 %distance from channel edge to gel edge

    %%Import measurements from fiji macro
    Iedge = xlsread('C:\path\ GelBG.csv',1,'B2:B241');%%Average Intensity at no-flux region
    Channel_Io = xlsread('C:\pathChannelBG.csv',1,'B2:B241'); %%Intensity within channel
    Igel=  xlsread('C:\path\GelNearChannelBG.csv','B2:B241');%%Average intensity of gel

    %% Convert slice/frame number to time interval
    Slice = xlsread('C:\path\Profile.csv','Profile','C1:IH1');
    Time_minute = Slice*.5;
    Time_second = Time_minute*60;

    %%Calculating C for each timepoint
    C_numerator=Iedge-Channel_Io;
    C_denominator = Igel-Channel_Io;
    C=C_numerator./C_denominator;

    %% Graphing logC versus time
    x = Time_second;
    y = C;
    plot=semilogy(x,y);

    %%Fit logC versus time to extract Lambda (slope)
    curvefit = fitlm(x,y,'poly1');
        coeff=curvefit.Coefficients.Estimate;
        Rvalue=curvefit.Rsquared.Ordinary;
        output = xlswrite('C:\path\curvefit.xlsx', coeff,1);

    %Use Lambda to calculate K (permeability) in microns/second
    Lamda = xlsread('C:\path\curvefit.xlsx',1,'A2:A2');
    K=(Dgelatin/Distance_microns)*(Lamda*tan(Lamda));
    K_cm = K*10000; %% conversion to cm/s
        outputValue = {;'K cm/s';'Lambda';'Rsquared'}
        values=[;K_cm; K;Lamda;Rvalue];
        result= table(outputValue, values);
        %Save results in excel file
        writetable(result,'C:\path\Results.xlsx','Sheet',1,'Range','A1:B3')
```